

Supplementary Information for

Vulnerability to helpless behavior is regulated by the circadian clock component CRYPTOCHROME in the mouse nucleus accumbens.

Alessandra Porcu^{1,2,3}, Megan Vaughan⁴, Anna Nilsson^{1,2,3}, Natsuko Arimoto², Katja Lamia⁴, David K. Welsh^{1,2,3}

¹Research Service, Veterans Affairs San Diego Healthcare System, San Diego, CA, USA

²Department of Psychiatry, University of California San Diego, La Jolla, CA, USA

³Center for Circadian Biology, University of California San Diego, La Jolla, CA, USA

⁴Department of Molecular Medicine, Scripps Research Institute, La Jolla, CA, USA

*Alessandra Porcu

Email: aporcu@health.ucsd.edu

This PDF file includes:

Supplementary text
Figures S1 to S9
Tables S1 to S2
SI References

Supporting Information Text

Materials and Methods

Mice

Circadian rhythms of clock gene expression were assessed in brain slices from male and female *mPeriod2-Luciferase* (PER2::LUC) knock-in mice 9-16 weeks old, maintained in 12:12 light/dark cycles (12 hours light, 12 hours dark). In these mice, the wild-type circadian clock gene *Period2* (*Per2*) has been replaced by homologous recombination with a construct incorporating the firefly *luciferase* (*Luc*) gene in tandem with wild-type *Per2*, such that a bioluminescent PER2::LUC fusion protein is expressed under control of all *Per2* regulatory elements (1). In our mice, the reporter

construct also incorporated an SV40 polyadenylation site to enhance expression levels (2), and mice were back-crossed to produce a congenic C57BL/6J background. Western blot and RNAscope assays were performed in male and female C57BL/6J mice 9-16 weeks old. *Cryptochrome* knock-down experiments were performed in Tg(Drd1a-cre)120Mxu (D1R-Cre) (3) and Tg(Drd2-cre)ER44Gsat (D2R-Cre) male and female mice 9-16 weeks old. Beginning 5 days before inescapable tail shock sessions, mice were singly housed with continuous access to water and food. We attempted to minimize the number of animals used, and to minimize animal pain and distress. Tail suspension and learned helplessness (LH) paradigms were used to measure helpless behavior, as previously described (4).

Tail suspension and learned helplessness tests

Our behavioral protocol (Figure 2A) consists of two training days and two testing days. At zeitgeber time 9 (ZT9, 9 h after lights on) on days 1-2, for inescapable tail shock (ITS) training, mice were restrained and received 120 electric tail shocks, each lasting 5 s, randomly timed within a 60 min session. Shock intensity was gradually increased from 0.25 to 0.60 mA: every 15 shocks, the current was increased by 0.05 mA. On day 3, at ZT9, mice completed the tail suspension test, in which they were observed for 6 min while gently held suspended by the tail. Total immobility time was recorded as a measure of helpless behavior. On day 4, at ZT13 (1 h after lights off), mice were transferred to shuttle boxes (San Diego Instruments, San Diego, CA, USA), and the learned helplessness test was performed under dim red-light conditions. Mice received 30 electric shocks to their feet through the grid floor of the shuttle box. During each test shock (0.10 mA, maximum duration 30 s) the gate between the two compartments remained open, and mice had a chance to escape the shock by crossing to the adjacent compartment. The schedule in trials #1-5 was fixed ratio (FR)-1 (crossing the gate once in order to escape the shock). In the remaining trials #6-30, the schedule was changed to FR-2 (crossing the gate twice in order to escape the shock). The number of escape failures and the escape latency were used as criteria for learned helplessness (LH) as described previously (5). In knockdown experiments, all behavioral tests started 3 weeks after AAV injections to allow time for full expression of shRNA. For the knockdown experiments, the tail suspension test was performed first, to assess helpless behavior before the two days of more stressful ITS training, followed by the LH test.

Brain slice culture and PER2::LUC measurements

PER2::LUC expression patterns were measured using a LumiCycle luminometer (Actimetrics, Wilmette, IL) as described previously (4). Using LumiCycle Analysis software (Actimetrics), PER2::LUC rhythm period, peak phase (acrophase), and amplitude were determined over 7 days by fitting a sine wave [Sin fit (Damped) for period, phase, and damping time (time to reach 1/e of initial amplitude), LM fit (Sin) for amplitude] to 24 h running average baseline-subtracted data. The first day of measurement was excluded from analyses. Amplitude was normalized to the total brightness in order to account for different sizes of brain tissue and technical differences between slices. Explants failing to show significant χ^2 periodogram values near 24 h (6) or a minimum of two PER2::LUC peaks were determined to be arrhythmic. Acrophase was defined as the time of the second PER2 peak.

Immunohistochemistry

For each brain, 6 slices encompassing the NAc were used for immunohistochemistry. Immunofluorescent labeling was performed in free-floating slices first blocked for 1h in 0.1 M phosphate buffer (PB) containing 3% normal horse serum (NHS) and 0.2% Triton X-100. After blocking, slices were incubated with antibodies against CRY2 (anti-Cry2-CT, 1:250, kind gift of Katja Lamia, Scripps Institute, USA) and/or c-Fos (1:200, Abcam 190289) and/or BMAL1 (7) (1:500, kind gift of David Weaver, University of Massachusetts, USA) in phosphate-buffered saline (PBS), 3% NHS, and 0.2% Triton X-100 for 24h at 4°C with constant shaking. After three washes in PBS, slices were incubated with fluorescent-tagged secondary antibodies (AlexaFluor anti-rabbit 647 nm, anti-guinea pig 555 nm), which were all used at 1:1000 dilution. Specificity of CRY2 (8) primary antibody was confirmed in brain slices from CRY2-knockout mice (Figure S9). Slices were washed and mounted in gelatin on glass slides, and cover slipped with Cytoseal mounting medium (Thermo Scientific). Images were taken with a Zeiss LSM800 confocal microscope. To quantify CRY2 expression, mean fluorescence was measured using ImageJ and background was subtracted.

RNAscope

The probe for *mCry1* (GenBank Accession Number AB000777) was designed to target nucleotides 1074–1793 of the cDNA sequence. The probe for *mCry2* (Gen Bank Accession Number AB003433) was designed to target nucleotides 1040–1649 of the cDNA sequence (9). Frozen brains were sectioned (30 µm) with a standard Leica Cryostat (CM1860). Fluorescent images of four NAc sections per mouse were acquired with a Zeiss LSM800 confocal microscope. Semi-quantitative histological scoring methodology based on ACD scoring criteria was used to quantify *Cry1* and *Cry2* expression. A score of 0 means no staining or less than 1 dot for every 10 neurons, whereas a score of 4 means greater than 15 dots per neuron or >10% dots in clusters.

Virus injection

Mice were anesthetized with 3% isoflurane and placed in a stereotactic apparatus (David Kopf Instruments, Model 900HD Motorized Small Animal Stereotaxic). Brain injections were performed during a continuous flow of 1% isoflurane. Bilateral stereotactic injection of AAV particles in the NAc was achieved according to atlas coordinates (Paxinos): antero-posterior 1.18 mm; mediolateral: 1.08 mm lateral; dorsoventral 4.91 mm. About 0.8 µl of virus was injected into each side of the NAc. For *Bmal1*-knockdown (*Bmal1*-KD), wildtype mice received a mixture of two shRNAs, either both *Bmal1* or both scrambled shRNAs. For *Cry1*- and *Cry2*-knockdown (*Cry*-KD): D1R-Cre or D2R-Cre mice received a mixture of two shRNAs, either both *Cry1* and *Cry2* shRNA AAV9 virus (>10¹³ GC/ml), or both scrambled shRNA AAV9 virus (>10¹³ GC/ml). To allow time for diffusion of the virus, the injection needle remained immobile for 8 minutes before removal. After surgery, mice were injected with 5 mg/kg/24 h Carprofen for analgesia. Efficiency of *Bmal1*-KD and *Cry*-KD was determined by immunofluorescence as shown in Figure 3 and 4.

Bioluminescence resonance energy transfer (BRET)

CHO-K1 cells were transfected with plasmids encoding the D1 receptor, Gαs-Rluc, Gγ2-Venus, Gβ1-Flag, and either mCry1 and mCry2, or mCry1-ΔCCm and mCry2-ΔCCm. Six h after

transfection, cells were seeded into 96-well microplates (Costar Corning) coated with poly-L-ornithine hydrobromide (P3655, Sigma-Aldrich). Forty-eight h after transfection, and following 10 min of incubation with the luciferase substrate (5 mM, Coelenterazine-h, Invitrogen), measurement was initiated using a Cytation T3MV microplate reader (BioTek Instruments). Then, after 29 cycles of BRET reading (~80 s), 10 μ M A68930 (Tocris) was applied to CHO-K1 cells. Luminescence and fluorescence signals were detected sequentially with an integration time of 200 ms. The BRET ratio was calculated as the ratio of light emitted by Venus (530-570 nm) to the light emitted by RLuc (370-470 nm) and corrected by subtracting ratios obtained with the RLuc fusion protein alone. The curves were fitted using GraphPad Prism 8.0 ("plateau followed by one-phase decay"). Δ BRET was calculated as the difference between the basal level and the plateau of the BRET signal (10). The pEGFP-N-Drd1 plasmid was purchased from Addgene. The pCMV6-XL4-DRD1 (human dopamine receptor D1) was purchased from Origene. $G\alpha_s$ -RLuc, $G\gamma_2$ -Venus, $G\beta_1$ -Flag, and $G\gamma_2$ -HA (11, 12) were kind gifts of Bernhard Bettler (University of Basel, Switzerland). mCry1, mCry2 (13), mCry1- Δ CCm, mCry2- Δ CCm (14) were kind gifts of Marc Montminy (Salk Institute, San Diego, USA).

Human subjects and cell lines

Subjects 18-65 years old were recruited at McLean Hospital and Vanderbilt University (cases) and the surrounding community (healthy controls) by Drs. Bruce Cohen and Richard Shelton. MDD cases were typically identified while inpatients in a psychiatric unit. All subjects provided informed consent and were paid to participate. The cell samples were de-identified prior to use in this study. Subjects were evaluated with a structured interview (SCID-Mini for DSM-IV) to establish diagnosis. Clinical features including age of onset, psychiatric family history, dysphoric/euphoric mania, past suicide attempts, and alcohol/substance use history were extracted from the diagnostic interview. Subjects were excluded if they were medically ill or had a history of adverse events with skin biopsies. Age-matched controls were excluded for any psychiatric diagnosis or use of psychotropic medication. Fibroblast cell lines were established from skin biopsies from the buttock. At the time of experiments, cell lines had been passaged 3-10 times. Case-control matching was maintained during cell culture procedures and experiments. Luminometry and gene expression experiments were performed as previously described (15).

Human fibroblast culture and luminometry

For reporter gene assays in human fibroblasts, as described previously (15), cells were grown to confluence in 100 mm plates in standard culture medium [DMEM with 10% fetal bovine serum (FBS), glutamine, and antibiotics (penicillin, streptomycin, and amphotericin)]. After 2 days, cells were dissociated with trypsin, and 10% of each culture was transferred into one of six identical 35 mm plates and stabilized for 48 h. Afterwards, cells were transduced with a lentiviral mouse *Per2* promoter-driven firefly luciferase (*Per2::luc*) circadian reporter construct. The transduction proceeded over 48 h as cells were grown to confluence (1.2×10^6 cells/plate). Immediately before luminometer assay, growth medium was replaced with HEPES-buffered, serum-free recording medium containing 1 mM luciferin (Biosynth International, Staad, Switzerland). This procedure was sufficient to synchronize *Per2::luc* rhythms without serum shock. Rhythm measurements were conducted in 35 mm culture plates as previously described (15) using a 32-well LumiCycle

luminometer (Actimetrics, Wilmette, IL, USA). Photoemissions were measured from duplicate plates of each sample for 70 s, every 10 min, for 5 days. Temperature was maintained at 35°C.

Gene expression

For analyses of *Cry1*, *Cry2*, *Bmal1* and *Clock* mRNA expression, duplicate cultures were grown in six-well plates. RNA was prepared using a Qiagen (Hilden, Germany) RNeasy kit, following the manufacturer's instructions. Using a high-capacity reverse transcriptase kit, cDNA (750 ng) was synthesized by following the manufacturer's protocol. Taqman RT-PCR was conducted using a Bio-Rad CFX384 thermocycler with primers (Applied Biosystems, Foster City, CA, USA) targeting *Cry1*, *Cry2*, *Bmal1*, *Clock*, and *GAPDH*, a non-rhythmic control gene suitable for circadian rhythm studies (16). Gene expression was measured 16 hours (circadian time, CT16) and 24 (CT24) hours after serum shock and relative to *GAPDH* using the comparative Ct method (17). Circadian time points 16 and 24 were chosen based on rhythm peak/trough times in previous studies (18).

Supporting Figures

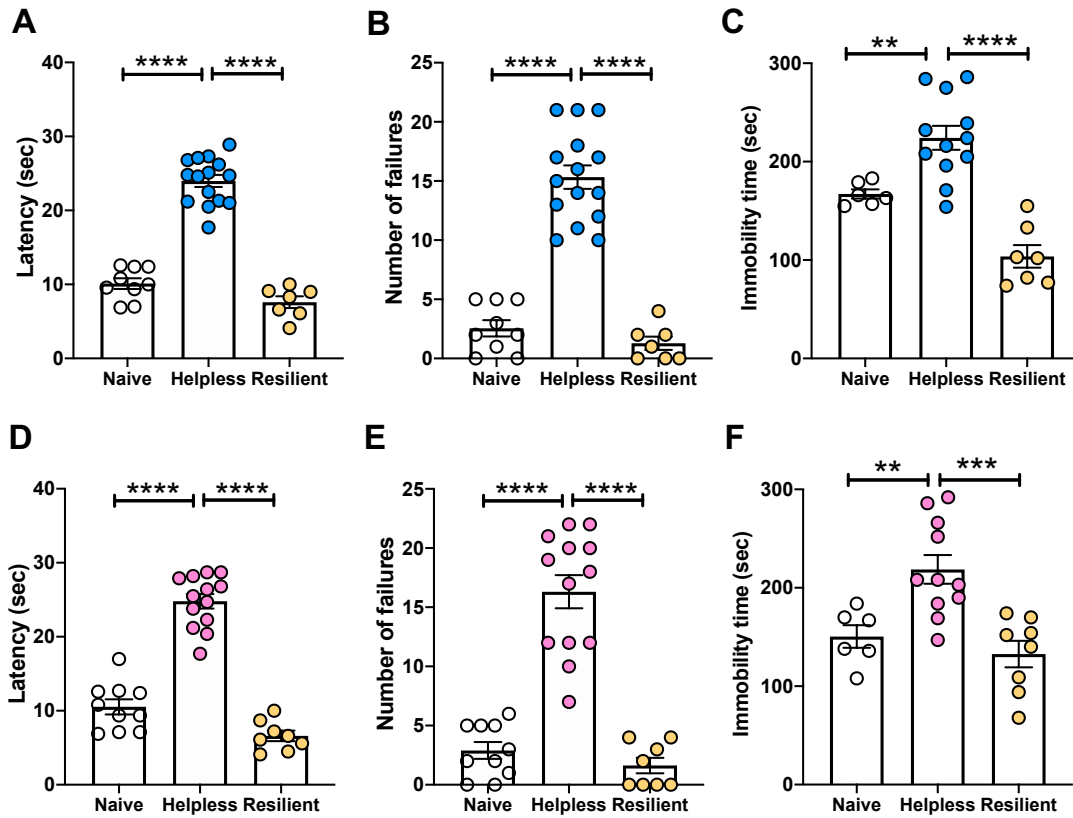


Figure S1. Inescapable tail shocks lead to helpless behaviors in both female and male mice. Bar graph shows escape latency of male (A) and female (D) mice, number of escape failures (B-E) and immobility time (C-F) of naïve (never received inescapable tail shock), helpless, and resilient mice. Male resilient (A-B-C) and female resilient (D-E-F) mice were defined as those showing escape latencies in the same range as naïve mice (white dots). Data are shown as means \pm SEM; ** $p < 0.01$, *** $p < 0.001$, **** $p < 0.0001$, one-way ANOVA with Bonferroni post-test. Each circle represents one mouse.

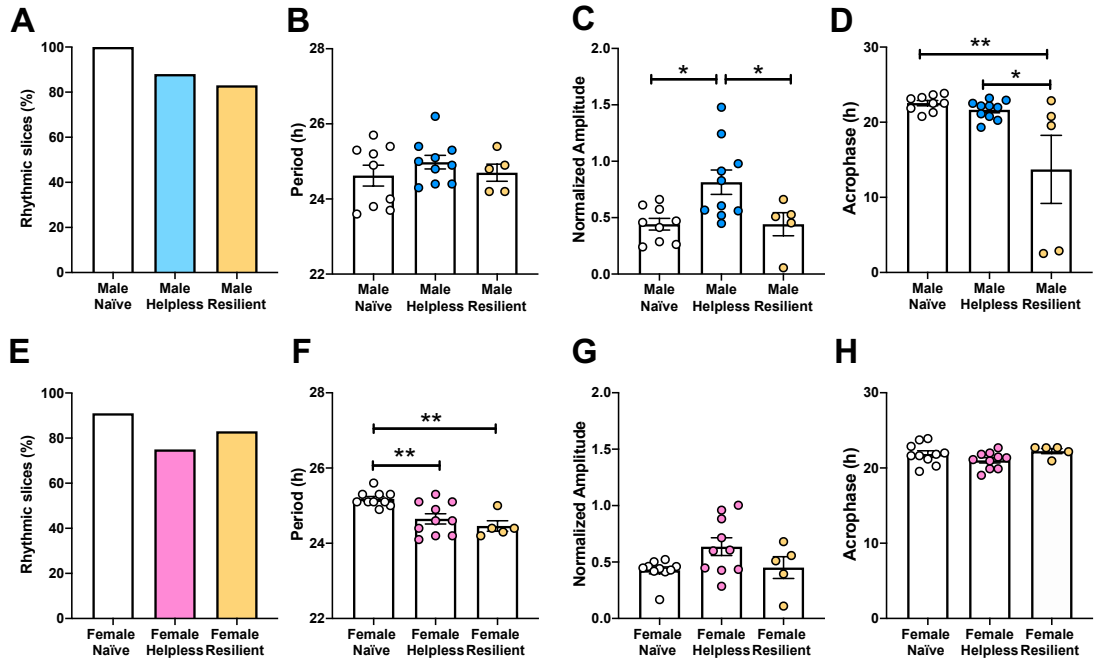


Figure S2. Helpless mice show altered PER2::LUC circadian rhythms in SCN. (A, E) SCN slices from naïve, helpless, or resilient male (A) or female mice (E) were reliably rhythmic regardless of behavioral state. Data are shown as percentages of slices showing significant PER2::LUC circadian rhythms. (B-D) SCN slices from male helpless mice showed increased rhythm amplitude in the SCN, and male resilient mice showed an earlier acrophase. (F-H) Female resilient and helpless mice showed shorter circadian rhythm period in the SCN, but no changes in rhythm amplitude or acrophase. Data are shown as means \pm SEM; * $p < 0.05$, ** $p < 0.01$, one-way ANOVA with Bonferroni post-test comparing all data sets within each sex. Each circle represents one mouse.

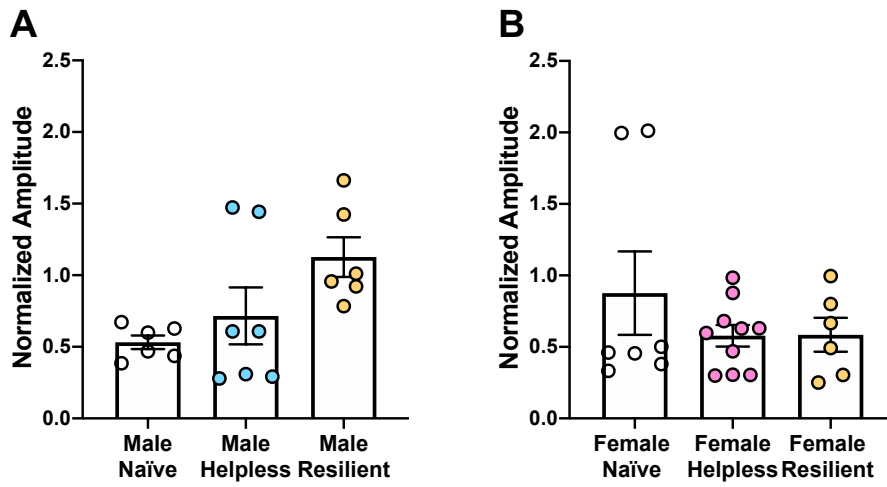


Figure S3. PER2::LUC amplitude in the NAc. NAc slices from helpless male (A) and female (B) mice showed no difference in rhythm amplitude compared to resilient and naïve mice. Data are shown as means \pm SEM. Each circle represents one mouse.

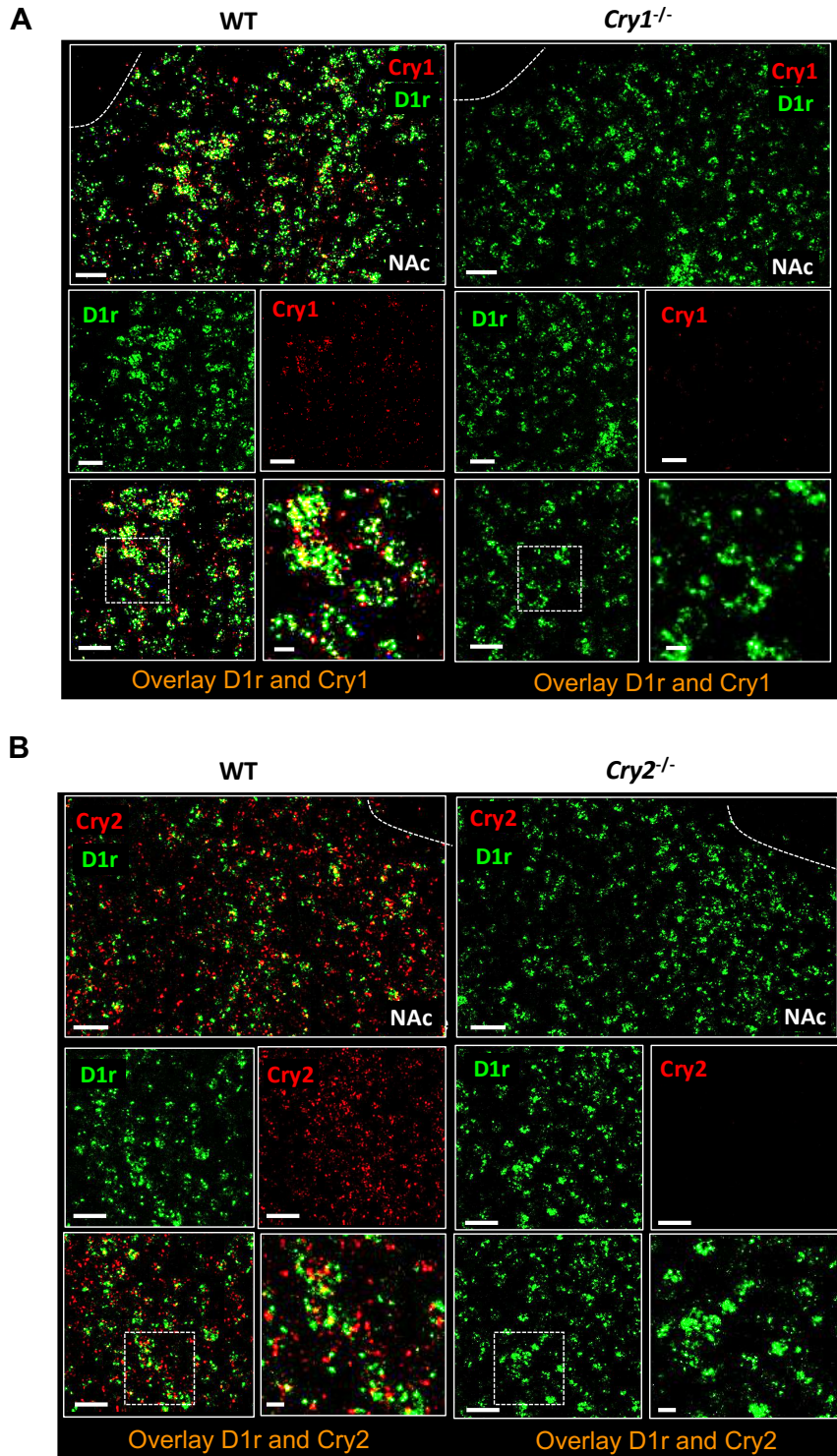
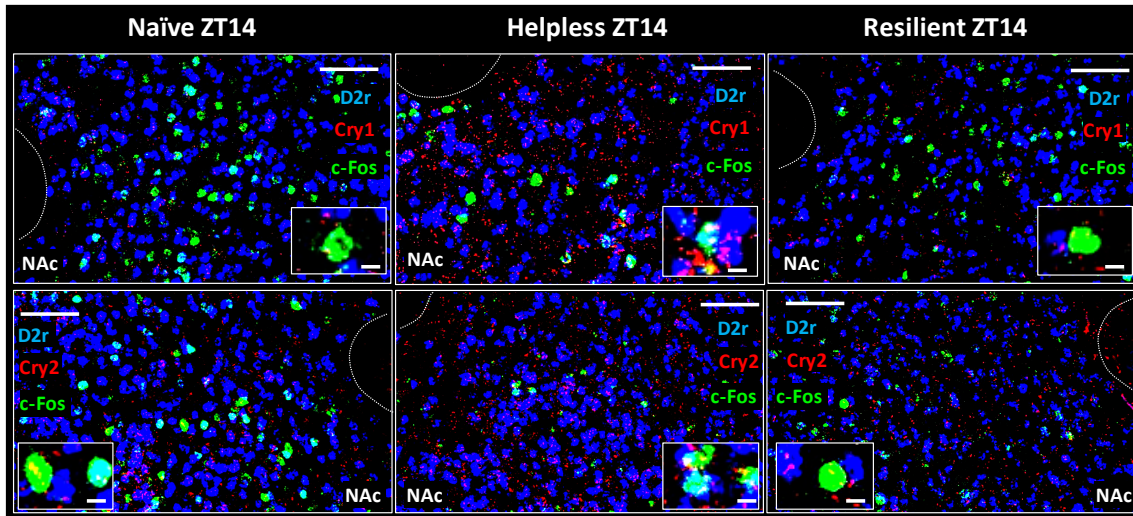


Figure S4. Validation of *Cry* probes for RNAscope in NAc of *Cry*-knockout mice. (A-B) Representative confocal micrographs showing *D1r* (green) and either (A) *Cry1* (red) or (B) *Cry2* (red) mRNA expression at ZT14 in the NAc of wildtype (WT) mice and either (A) *Cry1*-knockout (*Cry1^{-/-}*) mice or (B) *Cry2*-knockout (*Cry2^{-/-}*) mice. Scale bars for A and B: top 40 μ m, others 10 μ m.

A



B

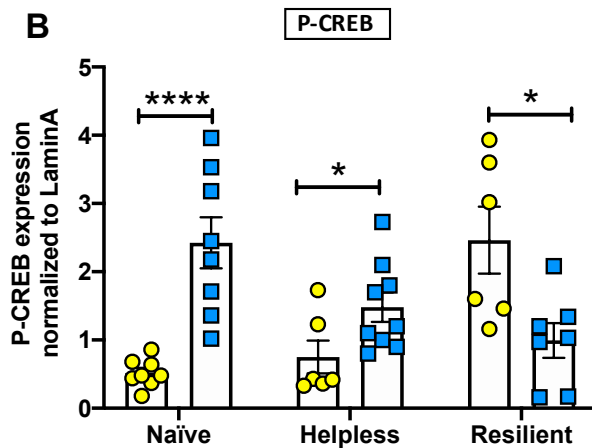


Figure S5. Helpless mice show higher D2R-MSN activation and an altered diurnal pattern of CREB activation in NAc. (A) Representative confocal micrographs showing *Cry1* (red, upper panel) or *Cry2* (red, lower panel) and *c-Fos* (green) mRNA expression detected by RNAscope in D2R-MSNs (dark blue, *D2r+*) at ZT14 in the NAc of naïve, helpless, and resilient mice. *c-Fos*/D2R+ co-expression is shown in light blue. Scale bars for each of the three behavioral states: top and bottom panels 100 μm , insets are shown at higher-magnification 10 μm . (B) Bar graph shows quantification of phospho-CREB (P-CREB) expression measured by western blot during the light phase at ZT5 (yellow circles) or the dark phase at ZT14 (blue squares), with different diurnal patterns in helpless vs. resilient mice. Data are shown as means \pm SEM. Student *t* test * $p < 0.05$, **** $p < 0.0001$. Each symbol represents one mouse.

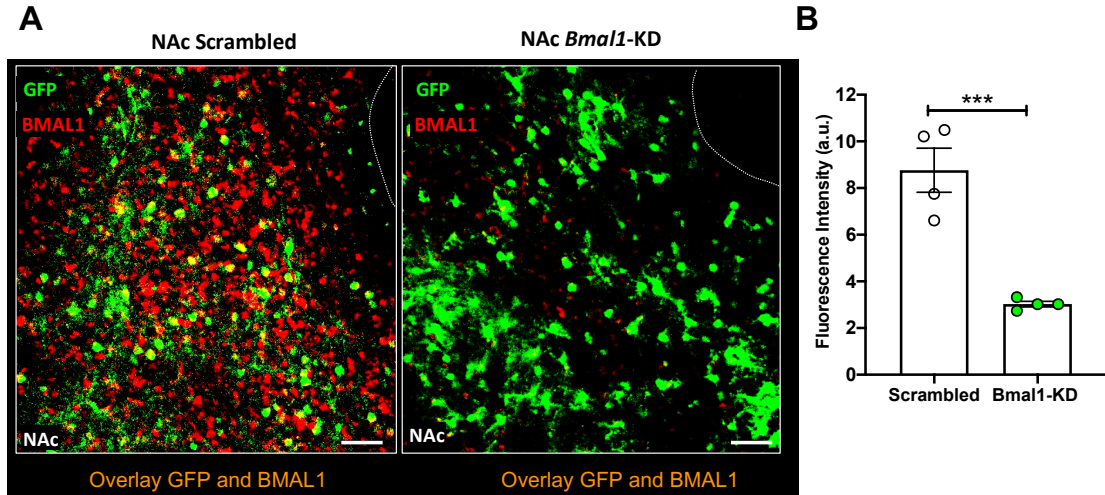


Figure S6. NAc of mice were injected with AAVs carrying *Bmal1*-knockdown (*Bmal1*-KD) or scrambled shRNA sequences as well as a GFP reporter. (A) Representative confocal micrographs of NAc from control mice (left) or mice injected with *Bmal1*-shRNA (right), showing transduced cells marked by GFP (green) and BMAL1 protein detected by immunolabeling (red). The overlays show that most cells transduced with *Bmal1*-shRNA show reduced BMAL1 expression. Scale bars: 100 μ m, except bottom right 20 μ m. (B) Bar graph shows quantification of BMAL1 immunofluorescence (arbitrary units), revealing an ~60% reduction of BMAL1 protein levels at ZT14, relative to control mice, in the NAc of mice injected with *Bmal1*-shRNA. Data are shown as means \pm SEM. Student *t* test *** p <0.001. Each symbol represents one mouse.

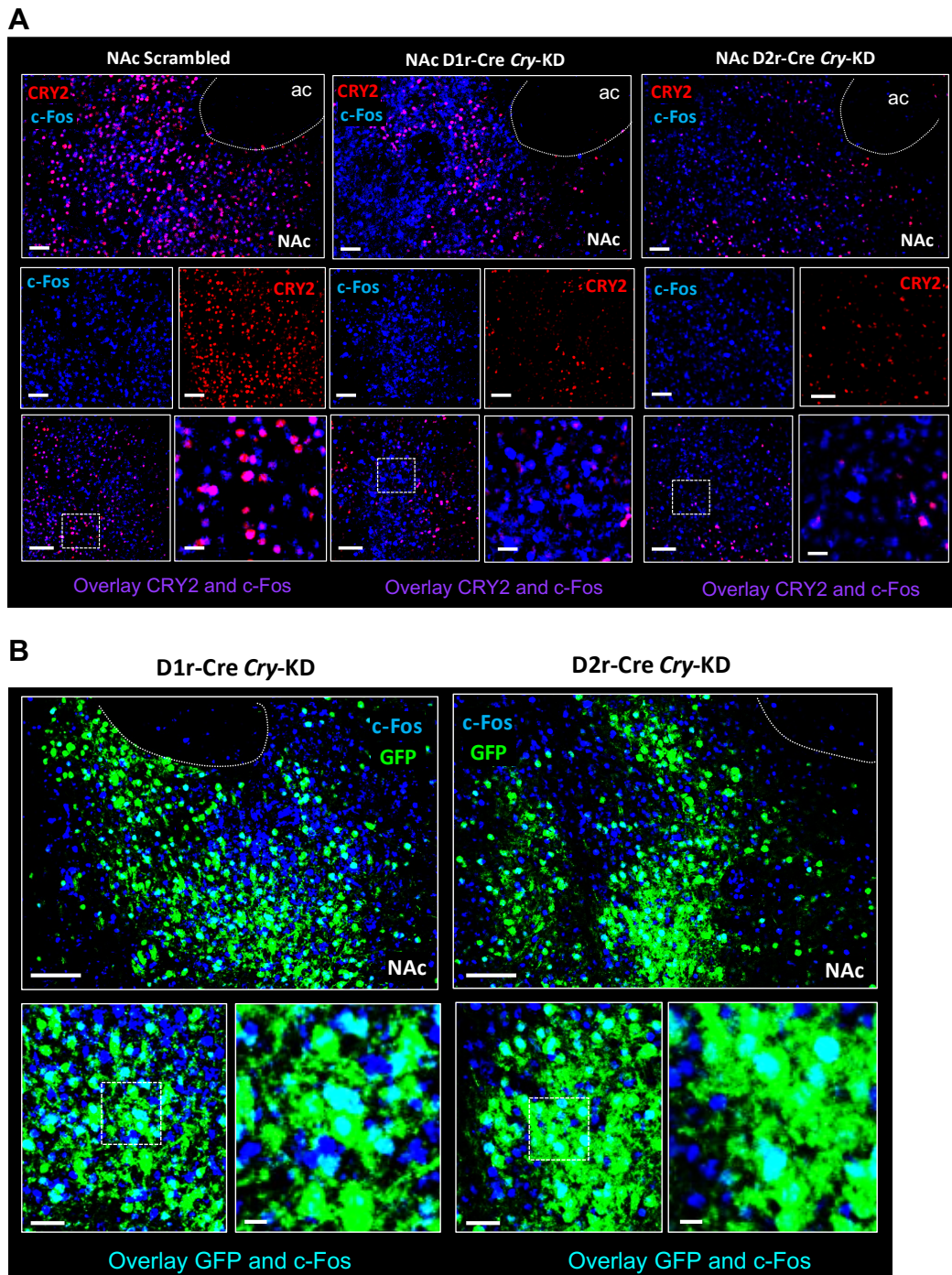


Figure S7. CRY2 and c-Fos expression in NAc after *Cry*-knockdown. (A) Representative confocal micrographs of NAc showing CRY2 and c-Fos expression detected by immunolabeling in control mice (left), D1r-Cre mice injected with *Cry*-shRNA (middle), and D2r-Cre mice injected with *Cry*-shRNA (right). For each condition, top panel shows co-expression in a large field of view, two

middle panels show c-Fos and CRY2 expression in a smaller field, bottom left panel shows co-expression in a smaller field, and bottom right panel shows an indicated portion of this panel at higher magnification. Scale bars: 50 μm , except bottom right 20 μm . (B) Representative confocal micrographs of NAc from D1r-Cre mice (left) or D2r-Cre mice (right) injected with *Cry*-shRNA, showing transduced cells marked by GFP (green) and c-Fos expression marked by immunolabeling (blue). For each condition, top panel shows co-expression in a large field of view, bottom left panel shows co-expression in a smaller field, and bottom right panel shows an indicated portion of this panel at higher magnification. Scale bars: top 100 μm , bottom left 40 μm , bottom right 10 μm .

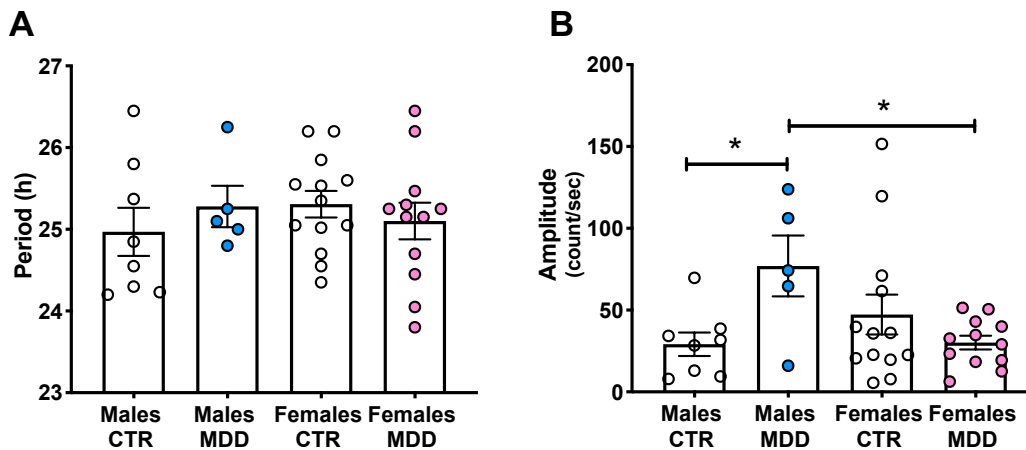


Figure S8. Fibroblasts from MDD patients show altered *Per2-luc* circadian rhythm amplitude. (A-B) Fibroblasts obtained from male or female healthy control subjects (CTR) or patients diagnosed with major depressive disorder (MDD) were transduced with a lentiviral *Per2-luc* circadian reporter. Rhythms were measured in a luminometer. No differences in circadian period were observed among the four groups. Cells from male MDD patients showed increased circadian rhythm amplitude (B) compared to female MDD patients or male controls. * $p < 0.05$, ** $p < 0.001$, one-way ANOVA with Bonferroni post-test. Each circle represents one subject.

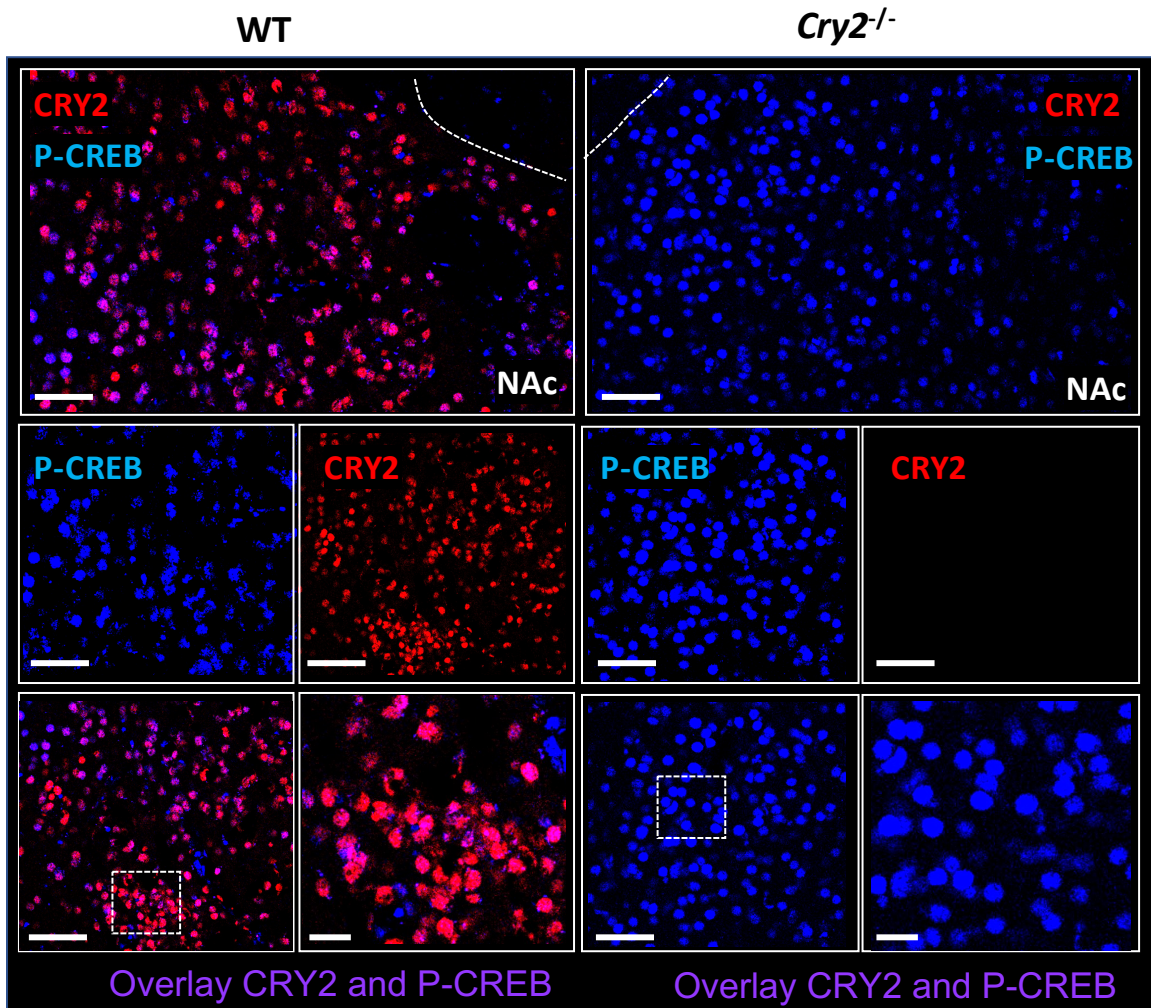


Figure S9. CRY2 antibody validation for immunofluorescence. Representative confocal micrographs showing CRY2 (red) and phospho-CREB (P-CREB) expression in the NAc of wildtype mice (WT) and *Cry2*-knockout mice (*Cry2*^{-/-}). Scale bars: top 50 μm, others 20 μm.

Table S1

Summary of western blot results shown in Figure 2B-C: CRY1 and CRY2 protein expression in the NAc of both female and male naïve, helpless, and resilient mice at ZT5 (light phase) and ZT14 (dark phase).

	n	ZT5 CRY1	ZT14 CRY1	ZT5 CRY2	ZT14 CRY2
Male Naïve	4	0.34 ± 0.02	3.39 ± 0.54	0.44 ± 0.03	2.62 ± 0.52
Male Helpless	4/5	2.57 ± 1.13	6.87 ± 1.88	2.18 ± 0.92	7.00 ± 1.44
Male Resilient	4	3.08 ± 1.19	4.28 ± 1.18	4.27 ± 1.18	3.90 ± 1.05
Female Naïve	3/4	0.50 ± 0.11	5.07 ± 0.92	0.23 ± 0.05	3.08 ± 0.38
Female Helpless	3/4	0.28 ± 0.06	6.42 ± 1.56	0.11 ± 0.06	5.60 ± 1.23
Female Resilient	3/4	2.05 ± 0.86	3.79 ± 1.07	3.55 ± 0.72	2.66 ± 0.83

Data are shown as means ± SEM. Numbers of mice (n) are indicated in the second column.

Table S2

Summary of RNAscope results shown in Figure 2E-F-G: *Cry1*, *Cry2* and *c-Fos* mRNA expression in D1r or D2r expressing neurons in the NAc of both female and male naïve, helpless, and resilient mice at ZT14 (dark phase).

	n	<i>Cry1</i> -D1r	<i>Cry2</i> -D1r	<i>Cry1</i> -D2r	<i>Cry2</i> -D2r	% <i>c-Fos</i> /D1r	% <i>c-Fos</i> /D2r
Male Naïve	4/5	2.27 ± 0.31	2.29 ± 0.21	2.12 ± 0.05	2.05 ± 0.18	63.5 ± 3.27	25.75 ± 3.47
Male Helpless	4/5	2.75 ± 0.08	3.13 ± 0.25	2.85 ± 0.05	3.18 ± 0.17	43.2 ± 6.37	52.00 ± 4.02
Male Resilient	3/4	2.16 ± 0.24	1.46 ± 0.03	2.00 ± 0.10	1.80 ± 0.21	67.7 ± 4.41	16.00 ± 3.05
Female Naïve	4/5	2.75 ± 0.38	1.93 ± 0.32	2.40 ± 0.18	1.70 ± 0.16	64.3 ± 3.21	21.25 ± 3.47
Female Helpless	4/5	3.20 ± 0.09	3.01 ± 0.35	2.93 ± 0.14	2.72 ± 0.17	59.5 ± 5.90	48.50 ± 7.62
Female Resilient	3/4	1.87 ± 0.24	1.50 ± 0.20	2.00 ± 0.20	1.75 ± 0.21	78.2 ± 4.76	17.00 ± 3.80

Data are shown as means ± SEM. Numbers of mice (n) are indicated in the second column.

SI References

1. S. H. Yoo, *et al.*, PERIOD2::LUCIFERASE real-time reporting of circadian dynamics reveals persistent circadian oscillations in mouse peripheral tissues. *Proc. Natl. Acad. Sci. U. S. A.* **101**, 5339–5346 (2004).
2. D. K. Welsh, S. Yoo, A. C. Liu, J. S. Takahashi, S. A. Kay, Bioluminescence Imaging of Individual Fibroblasts Reveals Persistent, Independently Phased Circadian Rhythms of Clock Gene Expression. *Curr. Biol.* **14**, 2289–2295 (2004).
3. J. Zhang, *et al.*, c-Fos facilitates the acquisition and extinction of cocaine-induced persistent changes. *J. Neurosci.* **26**, 13287–13296 (2006).
4. D. Landgraf, J. E. Long, D. K. Welsh, Depression-like behaviour in mice is associated with disrupted circadian rhythms in nucleus accumbens and periaqueductal grey. *Eur. J. Neurosci.* **43**, 1309–1320 (2016).
5. D. Landgraf, J. Long, A. Der-Avakian, M. Streets, D. K. Welsh, Dissociation of learned helplessness and fear conditioning in mice: A mouse model of depression. *PLoS One* **10**, 1–17 (2015).
6. P. G. Sokolove, W. N. Bushnell, The chi square periodogram: Its utility for analysis of circadian rhythms. *J. Theor. Biol.* **72**, 131–160 (1978).
7. J. LeSauter, *et al.*, Antibodies for assessing circadian clock proteins in the rodent suprachiasmatic nucleus. *PLoS One* **7** (2012).
8. M. D. & R. M. E. Katja A. Lamia, Stephanie J. Papp, Ruth T. Yu, Grant D. Barish, N. Henriette Uhlenhaut, Johan W. Jonker, Cryptochromes mediate rhythmic repression of the glucocorticoid receptor. *Nature* **480**, 22–29 (2011).
9. Y. Miyamoto, A. Sancar, Circadian regulation of cryptochrome genes in the mouse. *Mol. Brain Res.* **71**, 238–243 (1999).
10. C. Galés, *et al.*, Probing the activation-promoted structural rearrangements in preassembled receptor-G protein complexes. *Nat. Struct. Mol. Biol.* **13**, 778–786 (2006).
11. R. Turecek, *et al.*, Auxiliary GABAB receptor subunits uncouple G protein $\beta\gamma$ subunits from effector channels to induce desensitization. *Neuron* **82**, 1032–1044 (2014).
12. A. Porcu, *et al.*, Rimonabant, a potent CB1 cannabinoid receptor antagonist, is a Gai/o protein inhibitor. *Neuropharmacology* **133**, 107–120 (2018).
13. E. E. Zhang, *et al.*, Cryptochrome mediates circadian regulation of cAMP signaling and hepatic gluconeogenesis. *Nat. Med.* **16**, 1152–1156 (2010).
14. Pagkapol Pongsawakul, Regulation of Second Messenger Pathways by Cryptochrome (2013).
15. M. J. McCarthy, *et al.*, Genetic and clinical factors predict lithium's effects on PER2 gene expression rhythms in cells from bipolar disorder patients. *Transl. Psychiatry* **3**, e318-8 (2013).
16. R. Kosir, *et al.*, Determination of reference genes for circadian studies in different tissues and mouse strains. *BMC Mol. Biol.* **11** (2010).
17. T. D. Schmittgen, K. J. Livak, Analyzing real-time PCR data by the comparative CT method. *Nat. Protoc.* **3**, 1101–1108 (2008).

18. E. Nagoshi, S. A. Brown, C. Dibner, B. Kornmann, U. Schibler, Circadian gene expression in cultured cells. *Methods Enzymol.* **393**, 543–557 (2005).